CrystEngComm

Cite this: *CrystEngComm*, 2011, **13**, 5212

www.rsc.org/crystengcomm

**PAPER**

# Structure–property relations in chloroacetonitriles†

**Anna Olejniczak and Andrzej Katrusiak***

***Received 28th January 2011, Accepted 3rd May 2011***
**DOI: 10.1039/c1ce05144j**



The thermodynamic characteristics of acetonitrile, mono-, di- and tri- chloroacetonitriles have been rationalized in terms of molecular association and weak intermolecular forces. In this series acetonitrile and trichloroacetonitrile melt and boil at the lowest temperature and their enthalpies of vaporization are the lowest. The highest magnitudes of these parameters are those of monochloroacetonitrile. This trend coincides with the most balanced distribution of electrostatic potential (*i.e.* nearly equal magnitudes of the maximum and minimum potential) on the molecular surface for this compound. The chloroacetonitriles have been *in situ* pressure-frozen and their structures determined at room temperature by single-crystal X-ray diffraction at 1.30(5) GPa, 1.00(5) GPa and 0.90(5) GPa, for chloro-, dichloro- and trichloroacetonitrile, respectively. In their structures weak CH···N hydrogen bonds are gradually replaced by Cl···N and Cl···Cl interactions.

## Introduction

One of the best known structure–property relations in chemistry is that of the highest boiling point of water ($H_2O$), hydrogen fluoride (HF) and ammonia ($NH_3$) in the series of isoelectronic hydrides pointed out by Linus Pauling in his famous "The Nature of the Chemical Bond",[1] and since then repeated in many textbooks on chemistry as an argument for the existence of hydrogen bonds.[2] Meanwhile, the concepts of intermolecular interactions in molecular crystals evolved through the close packing approach described by Kitajgorodskij,[3] and most recently apart from the central dispersion forces more specific interactions between molecules have been identified.[4] These can be exemplified by halogen···halogen forces[5] and hydrogen bonds involving CH donors.[6] These bonds are much weaker than OH···O bonds in ice but they may afford explanation of specific syntons in the structures of molecular crystals. General and detailed knowledge on intermolecular interactions is of vital importance for predicting the molecular association and polymorphic behavior, and for designing structures of compounds or their mixtures of desired properties, such as solubility of pharmaceutical ingredients and solidification and vapor pressure of fuels. Intermolecular interactions with molecules of other compounds, in particular enzymes, proteins and biopolymers, are essential for the pharmaceutical activity of medicines. The molecules of organic compounds interact mainly *via* hydrogen bonds and other weak forces, commonly described as packing or van der Waals interactions. It was demonstrated that the molecular aggregation can be associated with the electrostatic potential and polarizability of the molecules,[5c,e,6d,7] rather than with the molecular dimensions only.[3] In this study we have investigated the hierarchy of intermolecular interactions in acetonitrile and its chlorine derivatives. In this series of compounds the H atoms are gradually replaced by Cl atoms, and the end-members' structures, acetonitrile and trichloroacetonitrile, are dominated by CH···N and halogen interactions, respectively. The role of –H, ≡N and –Cl atoms for the molecular aggregation has been compared and correlated with properties of these compounds, and the contribution of CH···N, CH···Cl, N···Cl and Cl···Cl interactions to the cohesion forces in the crystals has been assessed.

Chloroacetonitrile ($CH_2ClCN$), dichloroacetonitrile ($CHCl_2CN$) and trichloroacetonitrile ($CCl_3CN$) are chloro-derivatives of the simplest organic nitrile. They are widely applied, mainly in organic synthesis.[8] Their toxicity is intensely studied, as they are undesired side products of water chlorination.[9] The melting point of $CH_2ClCN$ is the highest (235 K), that of $CHCl_2CN$ is lower by 3 K and those of $CCl_3CN$ and acetonitrile ($CH_3CN$) and are still lower by 4 K and 7 K, respectively (Fig. 1). A similar but stronger dependence applies to the boiling temperature (355,[10] 399, 386 and 357 K for $CH_3CN$, $CH_2ClCN$, $CHCl_2CN$ and $CCl_3CN$, respectively) and freezing pressure. Thus the mp of $CCl_3CN$ and that of pure acetonitrile differ by merely 3 K only (the melting points are 231 K and 228 K, respectively), and the bp differ by 2 K. The enthalpies of vaporization for this series of acetonitriles exhibit an analogous dependence on molecular weight as the boiling points (Fig. 1), which is consistent with the Trouton's rule. We found that the freezing pressures at 296 K of $CCl_3CN$, 0.40(5) GPa, and of $CH_3CN$,[11] 0.38(5) GPa, are also similar. It is well known that freezing and boiling points can reflect the intermolecular

*Faculty of Chemistry, Adam Mickiewicz University, Grunwaldzka 6, 60-780 Poznań, Poland. E-mail: katran@amu.edu.pl; Fax: +48 61 829 1505; Tel: +48 61 829 1443*

† Electronic supplementary information (ESI) available: Selected crystal data and details of structure refinements. Shortest intermolecular distances in $CH_2ClCN$, $CHCl_2CN$ and $CCl_3CN$. CCDC reference numbers 751844–751846. For ESI and crystallographic data in CIF or other electronic format see DOI: 10.1039/c1ce05144j

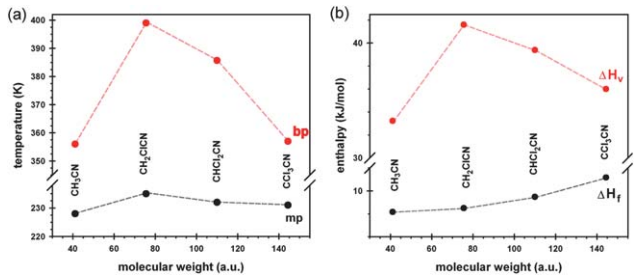


**Fig. 1** Ambient pressure (a) boiling and melting points, and (b) enthalpies of fusion ($\Delta H_f$) and vaporization ($\Delta H_v$) of chloric derivatives of acetonitrile plotted as the function of their molecular weight. The dashed lines joining the points have been drawn for guiding the eye only.

interactions, for example illustrating the effect of hydrogen bonds in hydrogen chalcogens.[1,2] In most compounds the increase in molecular weight usually leads to increase of both mp and bp, although some systematic differences depending *e.g.* on the parity of tether in *n*-diamines and *n*-diols[12] or molecular symmetry, *e.g.* in dichlorobenzenes,[13] are known. Crystal structures of two phases of $CH_3CN$, α stable between 228 and 201 K and β stable below 201 K (phases α and β exhibit a considerable hysteresis and transform between 201 and 222 K), were studied by several groups at 0.1 MPa.[14] Acetonitrile exhibits analogous phases α and β below and above 0.6 GPa, respectively.[11] However, no structures of chloroacetonitriles were determined, which could be connected with the vitrification observed both on cooling and pressurizing these compounds. Only $CCl_3CN$ in the gas phase was studied by electron diffraction.[15]

## Experimental

The chloric derivatives of acetonitrile were *in situ* pressure frozen in a modified Merrill–Bassett diamond-anvil cell (DAC).[16] All attempts to crystallize pure $CH_2ClCN$ by cooling and increasing pressure led to its vitrification. Therefore we proceeded with the crystallization from $CH_2ClCN$ : methanol 5 : 2 (v/v) mixture. After increasing its pressure to 1.30 GPa, the temperature was lowered to 230 K for a few minutes which triggered the formation of the polycrystalline mass. The single-crystal was grown by slowly heating and cooling the DAC (Fig. 2). The diffraction measurement was carried out at 1.30 GPa/296 K.

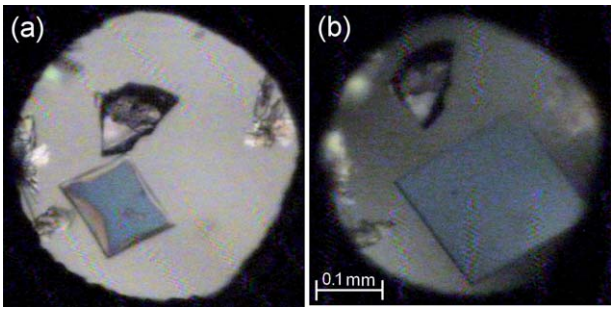


**Fig. 2** Two stages of isochoric growth of $CH_2ClCN$ single crystal from its methanol solution in the DAC chamber: (a) one single-crystal seed and (b) the single crystal used for the diffraction measurement at 1.30 GPa and 296 K. The ruby chip for pressure calibration is in the central upper part of the chamber, somewhat shifted upward in photograph (b).

Unlike $CH_2ClCN$, $CHCl_2CN$ and $CCl_3CN$ could be crystallized from neat samples: the freezing pressures of 0.70(5) GPa for $CHCl_2CN$ and 0.40(5) GPa for $CCl_3CN$ were measured when the crystals and liquid coexisted in the DAC at room temperature. The single crystals were obtained in the same manner by reducing the volume at isothermal conditions. To ensure stable orientation of the samples during the diffraction measurements, pressure was increased to 1.00 GPa for $CHCl_2CN$ (Fig. 3) and to 0.90 GPa for $CCl_3CN$ (Fig. 4).

The pressure in the DAC was calibrated by the ruby-fluorescence method,[17] using a Betsa PRL spectrometer, with an accuracy of 0.05 GPa. The single-crystal data have been measured with a KUMA KM4-CCD diffractometer. The CrysAlis software[18] was used for the data collections[19] and the preliminary reduction of the data. Reflection intensities were corrected for the effects of DAC absorption and sample shadowing by the gasket and the sample absorption,[20] and the reflections overlapped with diamond reflections have been eliminated. The symmetry could be unequivocally determined from systematic absences: space group *Pbca* for the $CH_2ClCN$ crystal at 1.30 GPa, space group $P2_1/c$ for $CHCl_2CN$ at 1.00 GPa, and $I4_1cd$ for $CCl_3CN$ at 0.90 GPa (Table 1). All structures were solved straightforwardly by direct methods,[21] and refined by full-matrix least-squares.[21]

Anisotropic temperature factors were generally applied for carbon, nitrogen and chlorine atoms, except $CHCl_2CN$ where only anisotropic chlorine atoms were retained due to the lowest crystal symmetry and the lowest completeness of the accessible diffraction data (Table 1). The H-atoms in the structures were calculated from molecular geometry ($d_{C-H} = 0.97$ Å), their $U_{iso}$'s constrained to 1.2 times $U_{eq}$ of the carrier atoms. The selected crystal data are listed in Table 1 (*cf.* Table S1† for experimental details) and the final models of the refined molecules are shown in Fig. 5.

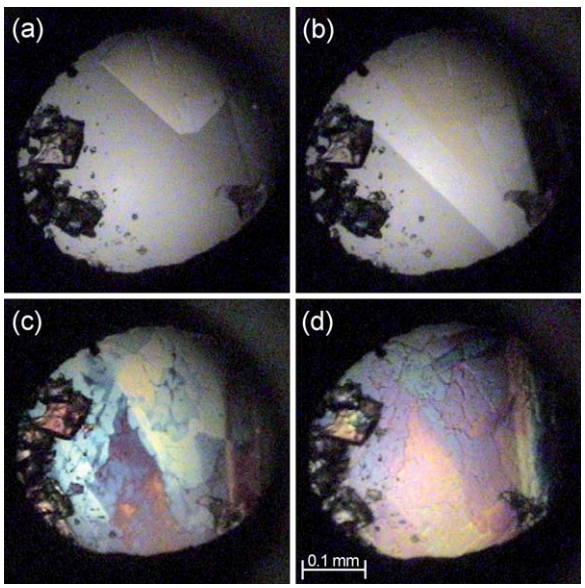


**Fig. 3** Isothermal growth of $CHCl_2CN$ single crystal viewed in polarized light: (a) and (b) one seed growing in the form of a plate; (c) almost the whole volume of high-pressure chamber filled by the sample, with visible defects on its surface; and (d) the sample at 1.00 GPa/296 K. Several ruby chips lie by the left edge of the gasket.

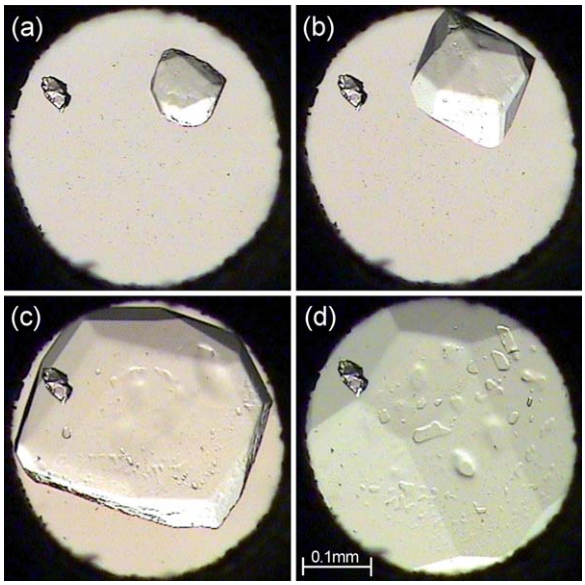


**Fig. 4** Stages of isothermal growth of a $CCl_3CN$ sample at 0.90 GPa/296 K (a), (b) and (c); and (d) this single crystal nearly fully filling the DAC. The ruby chip lies close to the top left edge of the gasket.

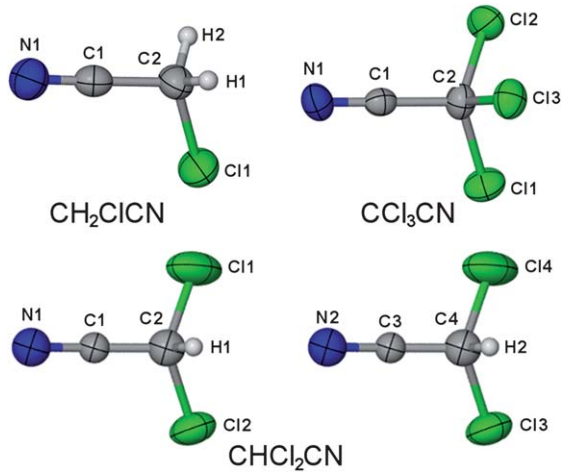


**Fig. 5** ORTEP drawings of the $CH_2ClCN$, $CHCl_2CN$ and $CCl_3CN$ molecules determined at high pressure. Thermal ellipsoids have been drawn at the 50% probability level (*cf.* Fig. S1†).

Structural drawings were prepared using the X-Seed interface of POV-Ray.[22] The *GAUSSIAN*03 program suite[23] and a PC were used to calculate the electrostatic potential on the molecular surface at the B3LYP/6-311G**(d,p) level of theory. Electrostatic potential was mapped onto the molecular surfaces defined as the 0.001 a.u. electron-density envelope.[24]

The differential scanning calorimetry (DSC) runs were recorded for the $CH_2ClCN$, $CHCl_2CN$ and $CCl_3CN$ samples enclosed in aluminium capsules on the DSC Q2000 V23.12 Build apparatus. The DSC thermographs were performed in the 93–470 K range with a rate 10 K $min^{-1}$.

## Results and discussion

### Gradual elimination of CH···N contacts

In the series of acetonitrile and its chloro-derivatives the intermolecular CH···N contacts are the shortest intermolecular contacts, relative to the sum of van der Waals radii[25] (1.70 Å for the C-atom, 1.20 Å for H, 1.55 Å for N). According to the H···N distances and C–H···N angle criteria these contacts (Table S2†) can be rather classified as electrostatic and dispersion interactions than weak hydrogen bonds. The CH···N contacts are gradually eliminated when the number of Cl atoms is increased. In the structures where there are both H and Cl atoms, CH···Cl contacts form a secondary motif, of contacts somewhat longer with respect to the sums of van der Waals radii[25] (1.75 Å for Cl). The shortest intermolecular distances in acetonitrile and its chloric derivates have been plotted in Fig. 6, and depicted on the Hirshfeld surfaces[26] (Fig. 7); the distances and angular dimensions of the shortest intermolecular contacts have been listed in the ESI in Tables S2–S4†.

In $CH_2ClCN$ the three shortest CH···N contacts (2.60 Å, 2.62 Å and 2.63 Å) arrange molecules into (001) sheets (Fig. 8), and the CH···Cl contacts are considerably longer (2.79 Å) and they are formed between the sheets. In $CHCl_2CN$ each symmetry-independent molecule is involved in two CH···N, one CH···Cl and one Cl···N contacts. Four short CH···N contacts of 2.39 Å,

**Table 1** Crystal data and structure refinements details for acetonitrile,[11] monochloro-, dichloro- and trichloroacetonitrile

| Compound | | α-$CH_3CN$[a] | β-$CH_3CN$[a] | $CH_2ClCN$ | $CHCl_2CN$ | $CCl_3CN$ |
|---|---|---|---|---|---|---|
| Pressure/GPa | | 0.57(5) | 1.50(5) | 1.30(5) | 1.00(5) | 0.90(5) |
| Temperature/K | | 296(2) | 296(2) | 296(2) | 296(2) | 296(2) |
| Crystal system | | Monoclinic | Orthorhombic | Orthorhombic | Monoclinic | Tetragonal |
| Space group | | $P2_1/c$ | $Cmc2_1$ | $Pbca$ | $P2_1/c$ | $I4_1cd$ |
| Unit cell dimensions/Å,° | $a$ | 3.9838(8) | 5.833(7) | 7.7821(16) | 5.9360(12) | 15.251(2) |
| | $b$ | 8.1352(16) | 5.082(2) | 7.0635(14) | 17.940(4) | 15.251(2) |
| | $c$ | 7.8165(16) | 7.563(5) | 11.620(2) | 7.5470(15) | 8.1219(16) |
| | $\beta$ | 99.33(3) | 90.00 | 90.00 | 92.44(3) | 90.00 |
| Volume/Å$^3$ | | 249.97(9) | 224.2(3) | 638.7(2) | 803.0(3) | 1889.0(5) |
| $Z/Z'$ | | 4/1 | 4/0.5 | 8/1 | 8/2 | 16/1 |
| Calculated density/g $cm^{-3}$ | | 1.091 | 1.216 | 1.570 | 1.819 | 2.031 |
| Completeness (%) | | 37 | 47.1 | 54.4/29.14 | 27.2/29.96 | 64.5/29.29 |
| Final $R_1/wR_2$ ($I > 2\sigma_1$) | | 0.0706/0.1656 | 0.0353/0.0757 | 0.0493/0.0995 | 0.0794/0.1439 | 0.0636/0.1613 |
| $R_1/wR_2$ (all data) | | 0.0818/0.1724 | 0.0369/0.0777 | 0.0580/0.1043 | 0.2091/0.1994 | 0.0707/0.1724 |

[a] According to ref. 11.

 

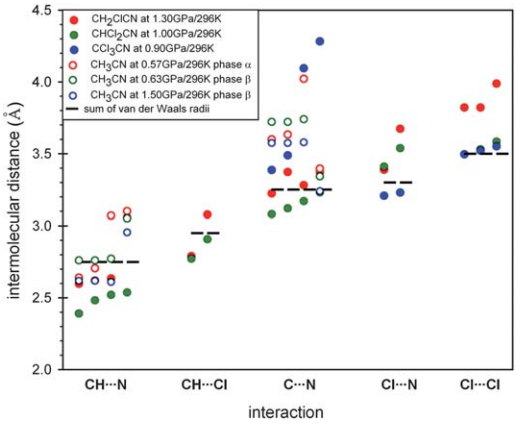


**Fig. 6** The intermolecular interactions of $CH_2ClCN$ at 1.30 GPa/296 K (red), $CHCl_2CN$ at 1.00 GPa/296 K (green) and $CCl_3CN$ at 0.90 GPa/296 K (blue) compared to those in $CH_3CN$ (open symbols); the sums of van der Waals radii[25] are indicated by the dashed lines. The estimated standard deviations of the distances are in the 0.01–0.03 Å range (*cf.* Tables S2 and S3†).

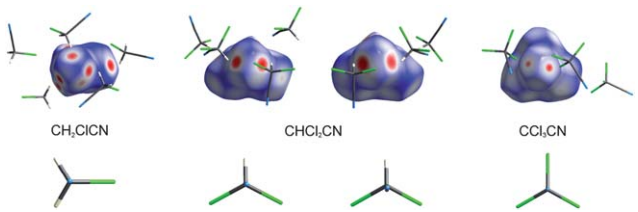


**Fig. 7** The molecular Hirshfeld surface of the chloric derivatives of acetonitrile decorated with the color scale depending on the intermolecular distances (normalized contact distance), and the closest molecules shown as the stick models: $CH_2ClCN$ at 1.30 GPa/296 K; two symmetry independent molecules of $CHCl_2CN$ at 1.00 GPa/296 K; and $CCl_3CN$ at 0.90 GPa/296 K. The surface regions forming intermolecular contacts shorter than the sums of their van der Waals radii are highlighted in red, longer contacts are in blue, and contacts around this sum are in white. The large stick models below the drawings show the orientation of molecules presented in the form of Hirshfeld surfaces.

2.48 Å, 2.52 Å and 2.54 Å link molecules along the (010) planes, and there are also CH···Cl contacts of 2.77 Å within so formed sheets (Fig. 8); between these sheets only weak Cl···Cl interactions are observed. The $CCl_3CN$ structure is governed by weak Cl···Cl interactions between the molecules forming chains down [001], and by weak Cl···N interactions. Unlike in $CH_2ClCN$ and $CHCl_2CN$ crystals, the $CCl_3CN$ molecules do not aggregate into distinct sheets. The weak Cl···Cl and Cl···N interactions in $CCl_3CN$ form a three-dimensional pattern shown in Fig. 8.

The Cl···Cl and Cl···N contacts are relatively long in the structure of $CH_2ClCN$ and become the shortest in the structure of $CCl_3CN$. In the structures with CH···N contacts, the molecular orientation is not optimum for interactions involving Cl atoms. Also, the CH···N contacts in $CHCl_2CN$ are shorter than in $CH_2ClCN$ (Tables S2 and S3†). Despite the considerable differences between the structures of $CH_2ClCN$ and $CHCl_2CN$, there are some similarities between the patterns of their intermolecular interactions. In both crystals the CH···N interactions aggregate molecules into sheets, with chlorine atoms directed outward. This behaviour is consistent with the halophobic properties of the chlorine atoms, as postulated by Grineva and Zorkii.[27] It further confirms that in these two structures interactions of Cl atoms are rather of secondary importance compared to CH···N. It thus appears that the contribution of CH···N interactions is the most important of all specific interactions for the molecular aggregation observed in these structures.

## Patterns of CH···N and CH···Cl contacts in $CH_3CN$, $CH_2ClCN$ and $CHCl_2CN$

In $CH_3CN$ phase α, two H-atoms (per molecule) participate in short CH···N contacts, whereas in phase β all three H-atoms form CH···N contacts of a similar distance (Fig. 9).[11,14] By adopting for CH···N contacts the terminology of hydrogen bonds, in $CH_2ClCN$, one of two H-atoms can be described as a three-centred CH···N bond, and the other as a four-centred (bifurcated) CH···N bond; and the N atom is the H-acceptor in these three H-bonds, like in β-$CH_3CN$ (Fig. 9). However, in $CH_2ClCN$ the C–H···N angles are smaller by 50° than in β-$CH_3CN$. Within the (001) sheets in $CH_2ClCN$, three types of CH···N bonded rings can be distinguished: $R_3^2$ (8), $R_2^2$ (8) and $R_2^2$ (4).[29] The pattern of $R_4^4$ (16) ring present in α-$CH_3CN$ can be also distinguished in $CH_2ClCN$, however it has been divided into three smaller rings, $R_2^2$ (8), $R_3^2$ (8) and $R_3^2$ (8) by two transannular CH···N hydrogen bonds. The H-bonding patterns in $CH_3CN$ and $CH_2ClCN$ are completed with similar $R_4^2$ (8) and $R_2^2$ (4) rings, respectively (Fig. 9).

The CH···N bonded sheets in the $CHCl_2CN$ crystal each involves both symmetry independent molecules. Each symmetry-independent H-atom forms a four-centered hydrogen bond. Dimensions of these two four-centered H bonds are similar. They have similar H···N distances and C–H···N angles. Thus it is evident that on decreasing the number of H-atoms in the chloroacetonitrile series, the H-atoms become increasingly involved in the formation of CH···N bonds. The CH···N hydrogen bonded pattern consists of $R_3^3$ (10) rings, each comprising both symmetry-independent molecules and two terminal groups of two other symmetry-independent molecules (Fig. 9).

## Structure–property relations

In chloroacetonitriles the intermolecular distances of CH···N and CH···Cl are the shortest contacts both in their absolute values and relative to sums of van der Waals radii[25] (Fig. 6). This coincides with the higher stability (higher melting and boiling points) of $CH_2ClCN$ and $CHCl_2CN$, compared to $CCl_3CN$. However it should be noted, that the comparison of the shortest contacts in $CH_2ClCN$ and $CHCl_2CN$ with their stability (Fig. 1) is inconsistent with this reasoning. Four CH···N contacts in $CHCl_2CN$ are shorter than three short contacts in $CH_2ClCN$, and two CH···Cl contacts in $CHCl_2CN$ are shorter than the two shortest contacts in $CH_2ClCN$, which do not correspond to the sequence of melting points and boiling points of these compounds. The CH···N and CH···Cl contacts in $CHCl_2CN$ are shorter than in $CH_2ClCN$, despite that the structure of $CHCl_2CN$ was determined at lower pressure than $CH_2ClCN$ (Table 1). Intermolecular contacts N···Cl in $CCl_3CN$ are markedly shorter than in other chloroacetonitriles (Fig. 6), and Cl···Cl contacts in $CHCl_2CN$ and $CCl_3CN$ are much shorter than in

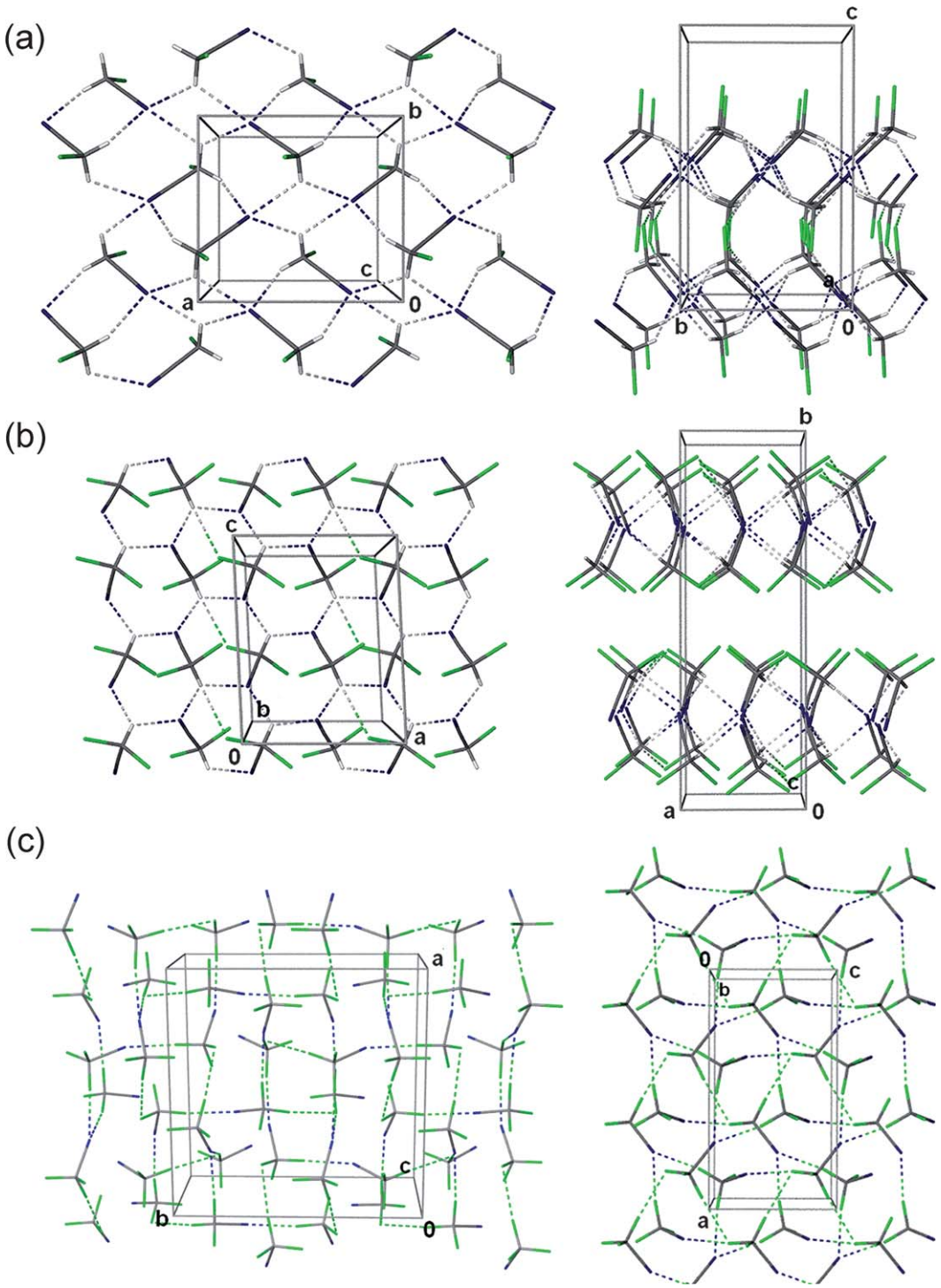


**Fig. 8** Autostereographic projections[28] of the molecular packing in: (a) $CH_2ClCN$ structure at 1.30 GPa/296 K; (b) $CHCl_2CN$ at 1.00 GPa/296 K; and (c) $CCl_3CN$ at 0.90 GPa/296 K. The shortest intermolecular contacts are indicated as the dashed lines. Two projections of $CH_2ClCN$ and $CHCl_2CN$ structures have been drawn to illustrate their CH···N bonded sheets.

$CH_2ClCN$. It is thus apparent that when the number of H atoms is becoming insufficient (for the formation of CH···N bonds) the interactions involving Cl-atoms become shorter and increasingly important for the molecular arrangement. In the structure of $CH_2ClCN$, governed mainly by CH···N contacts, there is one CH···Cl contact shorter than the sum of van der Waals radii,[25] whereas Cl···Cl and Cl···N distances are all longer than the sums of appropriate radii. It can be observed that most of the shortest intermolecular distances are reversely proportional to molecular weight (Fig. S2†). For example, the shortest of N···H contacts is present in $CHCl_2CN$, and the shortest Cl···N contact exists in $CCl_3CN$.

 

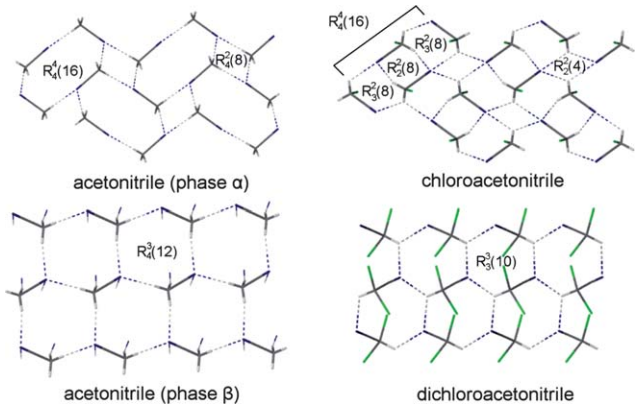


**Fig. 9** Comparison of hydrogen-bonding patterns in α-$CH_3CN$, β-$CH_3CN$, $CH_2ClCN$ and $CHCl_2CN$ (*cf.* Fig. 8).

Finally, it was shown recently[7g,i] that there is a considerable electrostatic contribution to the cohesion forces of molecular crystals, like in ionic crystals. The $CH_3CN$ molecule is strongly polarized along its molecular axis ($\mu = 13.17 \times 10^{-30}$ C m, Fig. 10), and the dipole moment of $CH_2ClCN$, $CHCl_2CN$ and $CCl_3CN$ decreases to $10.97 \times 10^{-30}$ C m, $8.57 \times 10^{-30}$ C m, and $6.92 \times 10^{-30}$ C m, respectively. The $CH_3CN$ molecule has the lowest magnitude of electrostatic potential on the nitrogen-atom surface, of −161 kJ mol$^{-1}$, compared to −135 kJ mol$^{-1}$, −118 kJ mol$^{-1}$, and −111 kJ mol$^{-1}$ for $CH_2ClCN$, $CHCl_2N$ and $CCl_3CN$, respectively. The highest electrostatic potential is located at the hydrogen atoms, and at the tips of Cl atoms in $CCl_3CN$. The highest electrostatic potential of $CH_3CN$, $CH_2ClCN$, $CHCl_2N$ and $Cl_3CN$ is 115 kJ mol$^{-1}$, 148 kJ mol$^{-1}$, 170 kJ mol$^{-1}$, and 98 kJ mol$^{-1}$, respectively (Fig. 10 and 11). A rim of small negative electrostatic potential perpendicular to the C–Cl bond is present

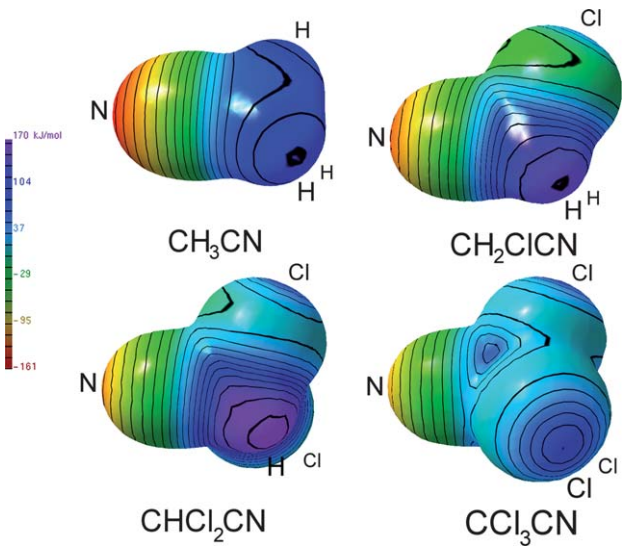


**Fig. 10** Calculated electrostatic potential in the color scale, ranging from −161 kJ mol$^{-1}$ (red) to 170 kJ mol$^{-1}$ (purple), mapped onto the molecular surface of acetonitrile and its chloric derivatives. The orientation of the molecules has been coordinated in this manner that the C≡N bond points to the left and one of the Cl–Cl bonds (C–H in acetonitrile) lies in the plane of the drawing and points up to the right.

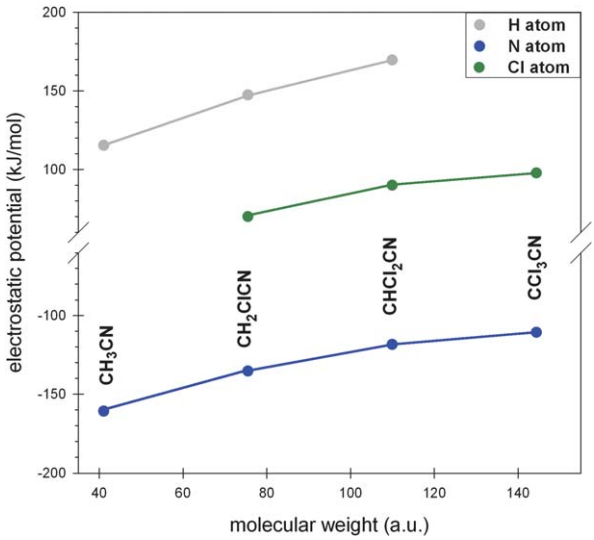


**Fig. 11** Maximum and minimum magnitudes of calculated electrostatic potential of hydrogen, nitrogen and chlorine atoms on the molecular surface of acetonitrile and its chloric derivatives (*cf.* Fig. 10). The lines have been drawn for guiding the eye only.

only in the $CH_2ClCN$ molecule. The magnitudes of electrostatic potential of chlorine atoms are much lower than those of nitrogen and hydrogen atoms, and for this reason electrostatic interactions of chlorine atoms in the structure are likely to be weaker than those of nitrogens and hydrogens.

### Molecular symmetry and space group relation

There are no apparent isostructural relations between the investigated acetonitrile and chloroacetonitrile crystals. These highly symmetric molecules are located at the general position in the crystals (α-$CH_3CN$, $CH_2ClCN$, $CHCl_2CN$ and $CCl_3CN$), and only in β-$CH_3CN$ the molecules assume the crystallographic mirror-plane symmetry. No trigonal crystals were formed, despite the $C_{3v}$ molecular symmetry of $CH_3CN$ and $CCl_3CN$. On the other hand, $CCl_3CN$ forms tetragonal crystals of space group $I41cd$, a unique occurrence in the Cambridge Structural Database (CSD) of this space group for the crystal built of $C_{3v}$-symmetric molecules. Among 12 060 tetragonal crystals deposited in CSD the molecules and ions of trigonal symmetry appear sporadically, and tetragonal crystals of $C_{3v}$ symmetric molecules can be found, but of other space groups, *e.g.* $P4/ncc$. Some $C_{3v}$-symmetric molecules are prone to form crystals of hexagonal family, *e.g.* chloroform and bromoform,[7a] however there are compounds which form crystals of lower symmetry only, *e.g.* monoclinic and orthorhombic crystals of chlorotrimethylsilane[30] and methyl iodide.[7g]

## Conclusions

According to electrostatic potential on $CH_2ClCN$ and $CHCl_2CN$ molecular surfaces, the strongest electrostatic interactions involve CH···N atoms. The patterns of CH···N interactions lead to some similarities between the molecular arrangement in the structures of $CH_2ClCN$ and $CHCl_2CN$ with those in $CH_3CN$ phases α and β. With the decreasing number of H-atoms and increasing number of Cl atoms, the CH···N contacts are

gradually replaced by weak CH···Cl and Cl···Cl interactions. The shortest CH···N and CH···Cl distances in $CH_2ClCN$ and $CHCl_2CN$ are consistent with the magnitudes of electrostatic potential on the molecular surface. This correlates with the anomalous freezing points in the series of acetonitrile and its chloric derivatives, and also with their boiling points. The enthalpies of vaporization for this series of acetonitriles exhibit an analogous dependence on molecular weight as the boiling points (Fig. 1), which is consistent with the Trouton's rule. With increasing number of Cl atoms the CH···N bonds become shorter, which also applies to the CH···Cl and Cl···Cl contacts. The Carnelley's rule,[31] stating that the melting point is higher for the more symmetrical molecules, fails in this series of compounds, where the end members, $CH_3CN$ and $CCl_3CN$, have the highest point-group symmetry $3m$ ($C_{3v}$) and the lowest melting and boiling points. The best correlation between boiling and freezing points is with the electrostatic-potential distribution on the molecular surfaces. Although the maximum difference between the potential values on the H and N atoms is approximately equal for all these compounds, it is for $CH_2ClCN$ that the negative and positive potentials of H and N are similar in their absolute magnitudes, which increases the electrostatic contribution to the cohesion forces. The dipole–dipole interactions in $CH_2ClCN$ are optimum between antiparallel molecular pairs, present in this centrosymmetric structure. Moreover, in the $CH_3CN$, $CH_2ClCN$ and $CHCl_2CN$ series the number of the highest positively charged surface regions of the molecules decreases for the smaller number of H-atoms, which leads to the match between the numbers of H-donors and H-acceptors, and to the shortest H···N and C···N distances in $CHCl_2CN$ (see Table S2†). Thus it appears that the dependence of mp in the series of chloroacetonitriles results from the complex combination of intermolecular interactions (weaker for Cl atoms) and the molecular shape and weight. The similar and even stronger dependence of boiling points in this series may be an indication that intermolecular interactions similar to those in the solid state persist in the melts of these compounds, in an analogous way as the hydrogen bonds affect the vaporization of hydrogen compounds of the elements of groups 5A, 6A and 7A of the Mendeleev's Table.[1,2]

## Acknowledgements

This study was supported by the Foundation for Polish Science, Team program 2009-4/6. Dr Anna Olejniczak acknowledges the reception of scholarship START from the Foundation for Polish Science in 2011.

## Notes and references


1 L. Pauling, *The Nature of the Chemical Bond*, Cornell University Press, New York, 1960.

2 (*a*) F. A. Cotton and G. Wilkinson, *Advanced Inorganic Chemistry*, John Wiley&Sons Inc., New York, 1972; (*b*) F. M. Miller, *Chemistry: Structure and Dynamics*, McGraw-Hill Book Co., New York, 1984; (*c*) A. F. Wells, *Structural Inorganic Chemistry*, Oxford University Press, 1984; (*d*) F. A. Cotton, G. Wilkinson and P. L. Gaus, *Basic Inorganic Chemistry*, John Wiley & Sons, 1994; (*e*) Z. Gontarz and A. Górski, *Jednopierwiastkowe struktury chemiczne*, Wydawnictwa Naukowo-Techniczne, Warszawa, 1998; (*f*) C. E. Housecroft and A. G. Sharpe, *Inorganic Chemistry*, Pearson Education Limited, Edinburgh, 2001; (*g*) N. Wiberg, A. Holleman and E. Wiberg, *Holleman-Wiberg's Inorganic Chemistry*, Academic Press, London, 2001.

3 A. I. Kitajgorodskij, *Molekularnyje Kristally*, Nauka, Moscow, 1972.

4 G. R. Desiraju, *Crystal Engineering. The Design of Organic Solids*, Elsevier, 1989.

5 (*a*) G. R. Desiraju and R. Parthasarathy, *J. Am. Chem. Soc.*, 1989, **111**, 8725; (*b*) P. Metrangolo, H. Neukirch, T. Pilati and G. Resnati, *Acc. Chem. Res.*, 2005, **38**, 386; (*c*) F. Zordan, L. Brammer and P. Sherwood, *J. Am. Chem. Soc.*, 2005, **127**, 5979; (*d*) P. Metrangolo and G. Resnati, *Halogen Bonding Fundamentals and Applications*, Springer, Berlin, 2008; (*e*) G. M. Espallargas, L. Brammer and P. Sherwood, *Angew. Chem., Int. Ed.*, 2006, **45**, 345.

6 (*a*) G. R. Desiraju, *Acc. Chem. Res.*, 1991, **24**, 290; (*b*) G. R. Desiraju, *Acc. Chem. Res.*, 1996, **29**, 441; (*c*) V. R. Thalladi, H.-C. Weiss, D. Bläser, R. Boese, A. Nangia and R. Desiraju, *J. Am. Chem. Soc.*, 1998, **120**, 8702; (*d*) G. R. Desiraju and T. Steiner, *The Weak Hydrogen Bond*, Oxford University Press Inc., New York, 1999; (*e*) A. Katrusiak, M. Podsiadło and A. Budzianowski, *Cryst. Growth Des.*, 2010, **10**, 3461.

7 (*a*) K. F. Dziubek and A. Katrusiak, *J. Phys. Chem. B*, 2008, **112**, 12001; (*b*) A. Olejniczak, A. Katrusiak and A. Vij, *CrystEngComm*, 2009, **11**, 1073; (*c*) A. Olejniczak, A. Katrusiak and A. Vij, *CrystEngComm*, 2009, **11**, 1240; (*d*) A. Olejniczak, A. Katrusiak, P. Metrangolo and G. Resnati, *J. Fluorine Chem.*, 2009, **130**, 248; (*e*) M. Podsiadło and A. Katrusiak, *CrystEngComm*, 2009, **11**, 1391; (*f*) K. Dziubek, M. Podsiadło and A. Katrusiak, *J. Phys. Chem. B*, 2009, **113**, 13195; (*g*) M. Podsiadło and A. Katrusiak, *CrystEngComm*, 2009, **11**, 1951; (*h*) M. Podsiadło and A. Katrusiak, *J. Phys. Chem. B*, 2008, **112**, 5355; (*i*) M. A. Spackman, J. J. McKinnon and D. Jayatilaka, *CrystEngComm*, 2008, **10**, 377.

8 (*a*) T.-L. Ho and C. M. Wong, *J. Org. Chem.*, 1973, **38**, 2241; (*b*) S. M. Sherif and A. W. Erian, *Heterocycles*, 1996, **43**, 1083; (*c*) J. P. Jayachandran, T. Balakrishnan and M.-L. Wang, *J. Mol. Catal. A: Chem.*, 2000, **152**, 91; (*d*) I. Vágó and I. Greiner, *Tetrahedron Lett.*, 2002, **43**, 6039; (*e*) A. G. Jamieson and A. Sutherland, *Tetrahedron*, 2007, **63**, 2123; (*f*) C. Rondot, P. Retailleau and J. Zhu, *Org. Lett.*, 2007, **9**, 247.

9 (*a*) A. E. Ahmed, S. Jacob and A. M. Nouraldeen, *J. Biochem. Mol. Toxicol.*, 1999, **13**, 119; (*b*) A. M. Mohamadin and A. B. Abdel-Naim, *Pharmacol. Res.*, 1999, **40**, 377.

10 Aldrich Advancing Science 2005–2006 Poland, Sigma–Aldrich Corporation, 2005.

11 A. Olejniczak and A. Katrusiak, *J. Phys. Chem. B*, 2008, **112**, 7183.

12 V. R. Thalladi, R. Boese and H.-C. Weiss, *Angew. Chem., Int. Ed.*, 2000, **39**, 918.

13 M. Bujak, K. Dziubek and A. Katrusiak, *Acta Crystallogr., Sect. B: Struct. Sci.*, 2007, **63**, 124.

14 (*a*) M. J. Barrow, *Acta Crystallogr., Sect. B: Struct. Crystallogr. Cryst. Chem.*, 1981, **37**, 2239; (*b*) T. Brackmeyer, G. Erker, R. Fröhlich, J. Prigge and U. Peuchert, *Chem. Ber.*, 1997, **130**, 899; (*c*) R. Enjalbert and J. Galy, *Acta Crystallogr., Sect. B: Struct. Sci.*, 2002, **58**, 1005.

15 R. L. Livingstown, L. Page and C. N. R. Rao, *J. Am. Chem. Soc.*, 1960, **82**, 5048.

16 L. Merrill and W. A. Bassett, *Rev. Sci. Instrum.*, 1974, **45**, 290.

17 (*a*) G. J. Piermarini, S. Block, J. D. Barnett and R. A. Forman, *J. Appl. Phys.*, 1975, **46**, 2774; (*b*) H. K. Mao, J. Xu and P. M. Bell, *J. Geophys. Res.*, 1985, **91**, 4673.

18 Oxford Diffraction, *CrysAlis CCD, Data Collection GUI for CCD and CrysAlis RED CCD Data Reduction GUI, Versions 1.171.24 Beta*, Wrocław, Poland, 2004.

19 A. Budzianowski and A. Katrusiak, *High-Pressure Crystallography*, ed. A. Katrusiak and P. F. McMillan, Kluwer Academic Publisher, Dordrecht, 2004, vol. 140, ch. 1, pp 101–112.

20 (*a*) A. Katrusiak, *REDSHABS*, Adam Mickiewicz University, Poznań, Poland, 2003; (*b*) A. Katrusiak, *Z. Kristallogr.*, 2004, **219**, 461.

21 G. M. Sheldrick, *Acta Crystallogr., Sect. A: Found. Crystallogr.*, 2008, **64**, 112.

22 (*a*) L. J. Barbour, *J. Supramol. Chem.*, 2001, **1**, 189; (*b*) *Persistence of Vision (TM) Raytracer, version 2.6*, Persistence of Vision Pty. Ltd., Williamstown, Victoria, Australia, 2004.

23 M. J. Frisch, et al., *GAUSSIAN03, Revision B.04*, Gaussian Inc., Pittsburgh, PA, 2003.


 

24 R. F. W. Bader, M. T. Carroll, J. R. Cheeseman and C. J. Chang, *J. Am. Chem. Soc.*, 1987, **109**, 7968.
25 A. Bondi, *J. Phys. Chem.*, 1964, **68**, 441.
26 (*a*) J. J. McKinnon, M. A. Spackman and A. S. Mitchell, *Acta Crystallogr., Sect. B: Struct. Sci.*, 2004, **60**, 627; (*b*) S. K. Wolff, D. J. Grimwood, J. J. McKinnon, D. Jayatilaka and N. A. Spackman, *CrystalExplorer 2.0*, University of Western Australia, Perth, Australia, 2007.
27 (*a*) O. V. Grineva and P. M. Zorkii, *J. Struct. Chem.*, 2001, **42**, 16; (*b*) O. V. Grineva and P. M. Zorkii, *J. Struct. Chem.*, 2002, **43**, 995.
28 A. Katrusiak, *J. Mol. Graphics Modell.*, 2001, **19**, 363.
29 (*a*) M. C. Etter, *Acc. Chem. Res.*, 1990, **23**, 120; (*b*) M. C. Etter, J. C. MacDonald and J. Bernstein, *Acta Crystallogr., Sect. B: Struct. Sci.*, 1990, **46**, 256; (*c*) J. Grell, J. Bernstein and G. Tinhofer, *Acta Crystallogr., Sect. B: Struct. Sci.*, 1999, **55**, 1030.
30 R. Gajda, K. Dziubek and A. Katrusiak, *Acta Crystallogr., Sect. B: Struct. Sci.*, 2006, **62**, 86.
31 (*a*) R. J. C. Brown and R. F. C. Brown, *J. Chem. Educ.*, 2000, **77**, 724; (*b*) M. Bujak, K. Dziubek and A. Katrusiak, *Acta Crystallogr., Sect. B: Struct. Sci.*, 2007, **63**, 124.